2011 50th IEEE Conference on Decision and Control and
European Control Conference (CDC-ECC)
Orlando, FL, USA, December 12-15, 2011

Management and Control Strategy Study for a New Hybrid Wind Turbine System

Hao Sun, Xing Luo and Jihong Wang, *Senior Member, IEEE*

Abstract—**Electrical power generation from wind energy has been recognized as one of major realistic energy sources in CO_2 emission reduction worldwide. However, matching power generation with the load demand remains a great challenge, due to the nature of wind energy intermittency. The paper addresses this issue by developing a new system with the structure of a hybrid connection of the wind turbine and compressed air energy storage. A scroll air motor is adopted to serve as an "air-electricity transformer" to compensate the power output during the period of low wind speed. The paper reports our study in developing a suitable management and control strategy for this hybrid system. The mathematical model for the whole hybrid system is derived in the paper. To achieve steady power output, a multi-mode process control strategy is proposed combined with fuzzy logical pitch control and PI air pressure control. The simulation study has demonstrated that the proposed new hybrid wind turbine system is feasible and has potential for industrial applications.**

I. Introduction

In recent years, a significant development of wind power has been evidenced, in fact, the world market for wind turbines has shown a robust growth in the past year, with approximately 16 Gigawatts of new capacity added to the power network worldwide within the first half year of 2010 [1]. With the increased penetration rate of wind power, it has been recognized that one of the major challenges still remains, that is, wind intermittency that will lead to power output unexpected fluctuations, and it can also affect the wind turbine system operation, life expectance and mechanical structures [2]. Wide range of efforts has been made to improve the match between wind energy output and the load demand. For instance, 'Smart' energy grids, dynamic grids with improved metering and increased demand control, are expected to provide a possible solution through efficient load management by shifting the demand to the period of renewable generation in operation [3].

Generation of storable secondary energy carriers for decoupling the fluctuating supply might be a preferable alternative in renewable energy. With the added energy storage, the surplus wind energy can be converted to other form of storable energy and then the stored energy will be used to generation when the wind power available cannot satisfy the load demand. Apart from the pumped water, battery, hydrogen and capacitors, compressed air energy storage (CAES) is also a well known controllable and affordable technology [4] [5] [6]. In a CAES system, the excess power is used to compress air which can be stored in a vessel or a cavern. The energy stored in compressed air will be used to generate electricity when required.Compared with other types of energy storage schemes, CAES is proven more cost-effective with no chemical contamination to the environment.

In this paper, the hybrid system will adopt the scroll technology for energy conversion and the structure of the hybrid system is different from the conventional CAES system proposed previously. The scroll air motor will be connected to the wind turbine shaft through a mechanical transmission mechanism to provide assistant driving force to smooth the short term transient behaviour. Also, the compressed air energy storage can still be used to directly generate electricity. Due to the capacity of scroll air motors, the proposed structure is more suitable for smaller scale wind turbine power generation so the paper focuses on the power scale around 2kW. The proposed system structure is illustrated in Fig. 1. From the figure, it can be seen that the electrical and pneumatic parts are connected through a continuously variable transmission clutch. This will lead to a direct compensation of torque variation on the wind turbine shaft while the air motor driving force is engaged. In turn, this will alleviate the mechanical stress imposed onto the wind turbine.

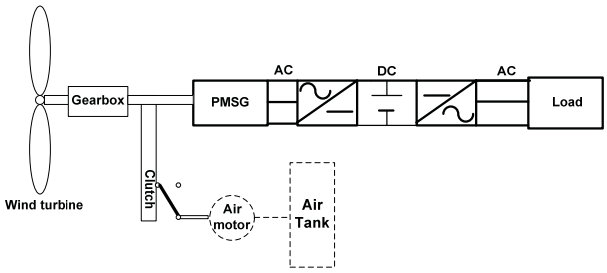

Figure 1: Small scale hybrid wind turbine with CAES

The detailed mathematical model for the whole system is derived, including a novel scroll-type air motor. To maintain a steady state power output while the wind speed varies, a multi-mode control strategy is proposed, in which fuzzy-logical pitch control is adopted during high wind speed without the CAES system and a PI control to regulate the air supply pressure is developed when wind speed is low and the air motor is engaged to the turbine shaft. Apart from the control strategy, it is required a good management system to determine when the air motor should be brought in and when it should be detached. With the combined decision making, management and control scheme, it has been shown that the

This work was supported in part by the Advantage West Midlands and the European Regional Development Fund for support of Birmingham Science City Energy Efficiency and Demand Reduction project.

Hao Sun, Xing Luo and Jihong Wang are with the School of Engineering, University of Warwick, Coventry, CV4 7AL, U.K. (Corresponding author: Jihong Wang, E-mail:jihong.wang@warwick.ac.uk).

proposed hybrid wind turbine system is feasible and the good control strategy is crucial for the whole system to work properly and efficiently.

II. Modeling Study of the Hybrid System

The proposed hybrid system consists of a typical wind turbine with permanent magnetic synchronous generator (PMSG), a scroll-type air motor and a mechanical power transmission system. The whole system mathematical model is described below.

A. Mathematical model of the wind turbine:

For a horizontal axis wind turbine, when a turbine works in steady states, the mechanical power output P is given by:

$$P = \frac{1}{2}\rho_a \pi r_T^2 V_w^3 C_p \tag{1}$$

where ρ_a is the air density, v_w is the wind speed, r_T is the blade radius. C_p reveals the capability of turbine for obtaining energy from wind. This coefficient depends on the tip speed ratio $\lambda=\omega_T r_T/ v_w$ and the blade angle, ω_T denotes the turbine speed. As this requires knowledge of aerodynamics, the computations are rather complicated. To simplify the description mathematically, numerical approximations have been developed [7]. In this paper, the following function is used to obtain the tip speed ratio,

$$C_p(\lambda,\theta) = 0.22\left(\frac{116}{\lambda_i} - 0.4\theta - 5\right)e^{\frac{-12.5}{\lambda_i}} \tag{2}$$

with

$$\frac{1}{\lambda_i} = \frac{1}{\lambda + 0.08\theta} - \frac{0.035}{\theta^3 + 1} \tag{3}$$

where θ represents the pitch angle. The above equations lead to the $C_p(\lambda, \theta)$ versus λ characteristics for various values of θ as depicted in Fig. 2. Using the actual values of the wind and rotor speed, which determine λ, and the pitch angle, the mechanical power extracted from the wind can be calculated using equations (1) to (3) [8].

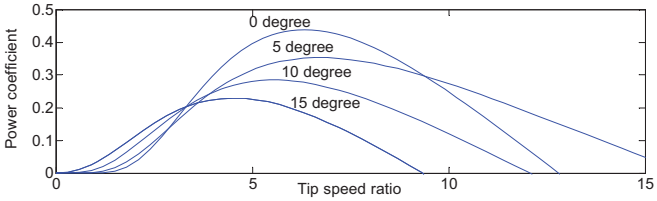

Figure 2: Power coefficient as a function of tip speed ratio and pitch angle

As shown in Figure 2, the power coefficient C_p varies with different values of the pitch angle (0^0, 5^0, 10^0, 15^0) and the best efficiency is obtained for $\theta=0^0$ in most cases [9]. A simplified drive train model in (4) is used to describe the dynamic behaviors of the wind turbine.

$$\frac{d}{dt}\omega_T = \frac{1}{J_T}(T_T - T_L - B\omega_T) \tag{4}$$

where J_T is the inertia of turbine blades, T_T and T_L stand for the torque of turbine and low speed shaft respectively, B is the damping coefficient of the driven train system.

B. Mathematical model of a permanent magnetic synchronous generator (PMSG)

In the paper, a resistance load only (for simplicity of analysis) is used for mathematical modelling of the PMSG and simulation study. The model is described below.

For the mechanical part:

$$\frac{d}{dt}\omega_G = \frac{1}{J_G}(T_G - T_e - F\omega_G) \tag{5}$$

$$\frac{d\theta_G}{dt} = \omega_G \tag{6}$$

The relationships linked through the electrical engineering principles are described in (7-11):

$$\frac{d}{dt}i_d = \frac{1}{L_d}v_d - \frac{R_s}{L_d}i_d + \frac{L_q}{L_d}p\omega_G i_q \tag{7}$$

$$\frac{d}{dt}i_q = \frac{1}{L_q}v_q - \frac{R_s}{L_q}i_q - \frac{L_d}{L_q}p\omega_G i_d - \frac{\varepsilon p\omega_G}{L_q} \tag{8}$$

$$T_e = 1.5p[\varepsilon i_q + (L_d - L_q)i_d i_q] \tag{9}$$

$$V_q = \frac{1}{3}[\sin(p\theta_G)\cdot(2V_{ab} + V_{bc}) + \sqrt{3}V_{bc}\cos(p\theta_G)] \tag{10}$$

$$V_d = \frac{1}{3}[\cos(p\theta_G)\cdot(-2V_{ab} - V_{bc}) - \sqrt{3}V_{bc}\sin(p\theta_G)] \tag{11}$$

where, θ_G and ω_G are the generator rotating angle and speed; F means the combined viscous friction of rotor and load; L is the inductance; R_S is the resistance of stator windings; p is the number of pole pairs of the generator; ε is the amplitude of the flux induced by the permanent magnets of the rotor in the stator phases; v means voltage; i is current with subscripts of a, b, c, d, q representing the axis of a, b, c, d, q for different electrical phases. The Park's transformation is employed for transforming X_{abc} (3-phase coordinates) to X_{dq} (DQ rotating coordinates) [10].

C. Mathematical model of a scroll-type air motor:

A scroll type air motor, also known as a scroll expander, is a relatively new concept to pneumatic actuators, which is essentially a refrigeration scroll compressor working backwards. A typical scroll air motor in motion is illustrated in Figure 4. It is shown that both scrolls are circular involutes with three wraps. The black scroll represents the moving scroll and the grey one is the fixed scroll. The moving scroll travels along the orbit anticlockwise when compressed air comes into Chamber 1 in the centre through the inlet. Each scroll is fitted to a back plate. As the moving scroll travels along the circular orbit, these two scrolls keep contacting at some points. Thus there is even number of crescent chambers. This unique structure features scroll air motors many advantages as well as higher ability of energy conversion than conventional pneumatic actuators, such as cylinders, vane-type air motors, etc [11].

Based on the previous work done by the authors' research group ([12][13]), a mathematical model of a simplified scroll air motor can be derived, with the following assumptions: no air leakage between chambers, using ideal compressed air, neglecting static frictions and working at a constant surrounding temperature.

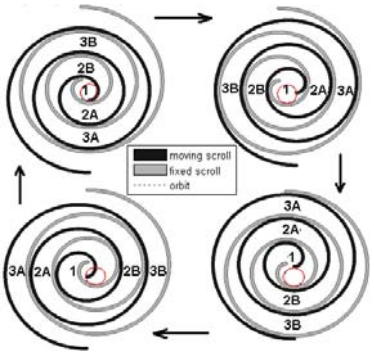

Figure 3: Schematic diagram of a scroll-type air motor

To obtain a complete mathematical model of a scroll air motor, the mechanical geometry features of a scroll air motor has been studied first. The scrolls' model can be derived from the fundamental geometry curve of a spiral. If the initial point of the spiral is at $\mathbf{A}_0 = (x_0, y_0)$ and the radius is defined by $\rho=\rho_0+\kappa\varphi$, each position of a point on the fixed scroll can be determined by

$$\mathbf{A}(\varphi) = \mathbf{A}_0 + \int_0^{\varphi}((\rho_0 + \kappa u)\cos u, (\rho_0 + \kappa u)\sin u)du \quad (12)$$

With its horizontal and the vertical position of

$$\begin{aligned} x_{\mathbf{A}}(\varphi) &= x_0 + (\rho_0 + \kappa\varphi)\sin\varphi + \kappa\cos\varphi - \kappa \\ y_{\mathbf{A}}(\varphi) &= y_0 - (\rho_0 + \kappa\varphi)\cos\varphi + \kappa\sin\varphi + \rho_0 \end{aligned} \quad (13)$$

where φ is the tangent angle of a point on the spiral, $\varphi \in [0, \varphi_s]$, $k=d_S/d\varphi$ determines the shape of a spiral.

While, the family of the moving scroll can be described by

$$\mathbf{A}(\varphi, \alpha) = \mathbf{A}(\varphi) + \mathbf{D}(\alpha) \quad (14)$$

Then we can derive the equations for the moving scroll:

$$\begin{aligned} x_{\mathbf{A}}(\varphi,\alpha) &= x_0 + (\rho_0 + \kappa\varphi)\sin\varphi + \kappa\cos\varphi - \kappa + r\sin\alpha \\ y_{\mathbf{A}}(\varphi,\alpha) &= y_0 - (\rho_0 + \kappa\varphi)\cos\varphi + \kappa\sin\varphi + \rho_0 - r\cos\alpha \end{aligned} \quad (15)$$

α is orbit angle of moving scroll in equation 14 and 15.

Applying Green's Theorem, the volume of the central chamber is given by

$$\begin{aligned} V_c(\alpha) = z[&(\kappa r - \kappa^2\pi - x_0 r + x_0\kappa\pi)\cos\alpha \\ &+ (\kappa r\rho_0\pi - r\rho_0 - y_0 r + y_0\kappa\pi)\sin\alpha \\ &+ (\kappa r\pi + 2\kappa\rho_0\pi)\alpha + \kappa^2\pi\alpha^2 - \kappa r + \frac{1}{3}\kappa^2\pi^3 \\ &- \frac{1}{2}\kappa r\pi^2 + \rho_0 r\pi + \frac{1}{2}r^2\pi + \rho_0^2\pi] \end{aligned} \quad (16)$$

where z stands for the depth of the scroll.

The area of one of the i^{th} (i=1, 2, 3…) i^{th} $(i = 1, 2, 3\cdots)$ pair of side chambers is:

$$V_s(\alpha, i) = \pi r^2 + 2\pi r(\rho_0 + \kappa(\alpha + \pi + 2(i-1)\pi)) \quad (17)$$

The volume of the exhaust chamber can be described by

$$V_e(\alpha) = V_{total} - V_c(\alpha) - V_s(\alpha) \quad (18)$$

where V_{total} stands for the total control volume of the scroll air motor.

Thus, we can get the pressures in different chambers:

In centre chamber,

$$\dot{P}_c = -\frac{\dot{V}_c}{V_c}\gamma P_c\omega_a + \frac{1}{V_c}\gamma RC_dC_0C_kA_ip_sf(p_s/P_c)\sqrt{T_s} \quad (19)$$

In the first pair of side chambers,

$$\dot{P}_{s1} = -\frac{\dot{V}_{s1}}{V_{s1}}\gamma P_{s1}\omega_a \quad (20)$$

In the second pair of side chambers,

$$\dot{P}_{s2} = -\frac{\dot{V}_{s2}}{V_{s2}}\gamma P_{s2}\omega_a \quad (21)$$

In the exhaust chamber,

$$\dot{P}_e = -\frac{\dot{V}_e}{V_e}\gamma P_{s2}\omega_a + \frac{1}{V_e}\gamma Rc_dc_0c_kA_op_ef(p_e/P_{atm})\sqrt{T_s} \quad (22)$$

The torque generated by a scroll air motor is the sum of the torques on all driving segments, it can be derived as:

$$\begin{aligned} M = zr[&(2\rho_0 + 2k\alpha + k\pi)(P_c - P_{s1}) \\ &+ (2\rho_0 + 2k\alpha + 5\pi)(P_{s2} - P_{s1}) \\ &+ (2\rho_0 + 2k\alpha + 5\pi)(P_e - P_{s2})] \end{aligned} \quad (23)$$

where, P_s is the supply pressure; P_{atm} is the pressure of atmosphere; Ts is the surrounding temperature; R, C_d, C_0 , C_k are air constant; $\gamma = 1.4$ is the ratio of specific heats; A_i, A_o are the effective area of inlet and outlet valves; r is the radius of the orbit; ω_a is the rotating speed of scroll air motor; f is a function of the ratio between the downstream and upstream pressures at the orifice.

D. Mathematical model of mechanical power transmission

The structure of the designed power transmission system is similar to that of a vehicular air conditioning system, which includes a clutch and a belt speed transmission to ensure coaxial running, as shown in Figure 4 [14].

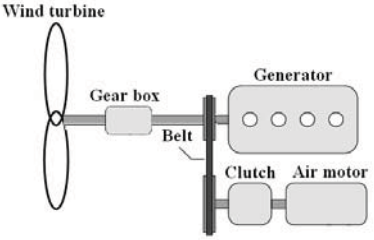

Figure 4: The structure of the power transmission system adopted in the hybrid wind turbine system

When the wind speed is low and the turbine cannot generate sufficient electricity to match the load, the compressed air in the air tank will be released into the scroll air motor through opening the pneumatic control valve; then the air motor will start rotating to be used to compensate the deficit of the power demanded. For the purpose of avoiding mechanical damage, the clutch will be engaged only when the turbine and the scroll air motor operates at the same speed. And the designed system must seek a proper approach to solve one more challenge during the engagement, that is, the speed of air motor could not match the speed of the turbine generator in most situations. Therefore, the two plates of the designed belt transmission have different diameters to play the function as a gearbox. When the pneumatic power compensation needs, the two situations of working states of the power transmission is described as follows:

Case I. Clutch disengaged: After the air motor has started during the period before the two sides of electromagnetic clutch get the same speed, the clutch can be considered completely separated. Considering friction and different payloads applying Newton's second law, we have,

$$M - M_f \omega_a = (J_a + J_f)\dot{\omega}_a \tag{24}$$

where J_a is the air motor inertia; J_f is the friction plate inertia; M is the drive torque; M_f is the friction coefficient; $\dot{\omega}_a$ represents the angular acceleration. Both the active plate and the passive plate of the belt transmission can be considered as an extra inertia load, so the total equivalent inertia will be:

$$J_{total} = J_{pass} + \varsigma^2 J_{act} \tag{25}$$

where J_{pass} and J_{act} are the inertias of the passive and active plate respectively, and ς is the speed ratio of the belt.

Case II. Clutch engaged: Once the angular velocity of air motor ω_a matches that of the active plate ω_G/ς, the clutch will be engaged with the two sides. After the engagement, the active plate and friction plate become the equivalent one mass. The dynamic equations are as follows:

$$\begin{cases} M - M_f \omega_a - T_{act} = (J_a + J_f + J_{act})\dot{\omega}_a \\ T_{pass} = \dfrac{T_{act}\eta}{\varsigma} \\ T_H + T_{pass} - T_e - F\omega_G = \dot{\omega}_G (J_G + J_{pass}) \\ \omega_a = \dfrac{\omega_G}{\varsigma} \end{cases} \tag{26}$$

where, T_H is the input torque of wind turbine high speed shaft, η is the transfer efficiency of the belt.

E. Overall state space model of the hybrid system:

Choose system state variables to be x_1: pressure in centre chamber, x_2: pressure in the first pair of side chambers, x_3: pressure in the second pair of side chambers, x_4: pressure in exhaust chamber, x_5 generator rotor angle, x_6 generator angle velocity, x_7: current in d axis, x_8: current in q axis. And input variables u_1: pitch angle, u_2: supply pressure. Integrating the wind turbine, driven train and generator models, the state functions of the whole hybrid wind turbine system can then be described by:

$$\dot{x}_1 = -\frac{\dot{V}_c}{V_c}\gamma x_1 \frac{x_6}{\varsigma} + \frac{1}{V_c}\gamma R C_d C_0 C_k A_t u_2 f(u_2 / x_1)\sqrt{T_s}$$

$$\dot{x}_2 = -\frac{\dot{V}_{s1}}{V_{s1}}\gamma x_2 \frac{x_6}{\varsigma}$$

$$\dot{x}_3 = -\frac{\dot{V}_{s2}}{V_{s2}}\gamma x_3 \frac{x_6}{\varsigma}$$

$$\dot{x}_4 = -\frac{\dot{V}_e}{V_e}\gamma x_4 \frac{x_6}{\varsigma} + \frac{1}{V_e}\gamma R c_d c_0 c_k A_o x_4 f(x_4 / P_{atm})\sqrt{T_s}$$

$$\dot{x}_5 = x_6$$

$$\dot{x}_6 = \frac{1}{J_G + J_{pass} + J_T \frac{\eta^{'}}{\varsigma^{'2}} + (J_a + J_f + J_{act})\frac{\eta}{\varsigma^2}} [\frac{\eta^{'}}{2x_6}\rho\pi r^2 v_w^3 C_p(u_1)$$

$$- B\frac{\eta^{'} x_6}{\varsigma^{'2}} + \frac{\eta}{\varsigma}M - M_f \frac{\eta x_6}{\varsigma^2} - 1.5p(\varepsilon x_8 + L_d x_7 x_8 - L_q x_7 x_8) - F x_6]$$

$$\dot{x}_7 = \frac{v_d}{L_d} - \frac{R_s}{L_d}x_7 + \frac{L_q}{L_d}p x_6 x_8$$

$$\dot{x}_8 = \frac{v_q}{L_q} - \frac{R_s}{L_q}x_8 - \frac{L_d}{L_q}p x_6 x_7 - \frac{\varepsilon p x_6}{L_q}$$

where, $\eta^{'}$, $\varsigma^{'}$ is the efficiency and speed ratio of wind turbine gearbox. With such a complicated structure of the system model, sometimes, it is difficult to obtain accurate values of system parameters. Intelligent optimization and identification methods proved to be an effective method to tackle this challenging problem [15] [16]. The test system for the proposed hybrid system structure is under development in the authors' laboratory and the data obtained from the rig can be used to improve the model accuracy.

III. MULTI-MODE PROCESS CONTROL STRATEGY

Based on the above expression in Section II, the complete hybrid system contains multi-mode operations, as described in Fig. 5, in which Mode 1 is for normal wind turbine operation, and Mode 2 corresponds to Case I, and Mode 3 to Case II. Therefore, to ensure the power output to match the load demand and stable, a suitable management or decision making strategy is essential and a multi-mode control is required to cover all the operation modes.

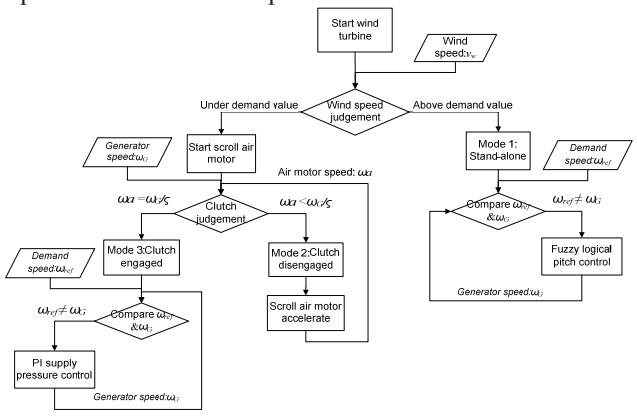

Figure 5: The multi-mode process diagram

In this paper, fuzzy logical pitch control is adopted in Mode 1, while PI air pressure control is used in Mode 3. Pitch angle control is the most common means to control the aerodynamic power generated by the wind turbine rotor. The developed control system has integrated a fuzzy logical controller for speed control of the generator that can limit the captured energy at high wind speeds. Fuzzy control provides a systematic way to incorporate human experience about how to control a nonlinear system, which usually has uncertain factors and inaccurate property. The controller is structured under Simulink environment, as shown in Fig. 6:

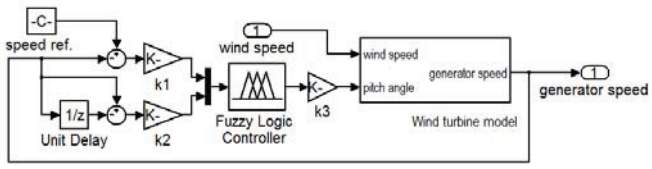

Figure 6: Fuzzy logical pitch controller diagram

Choosing the speed error V_e (difference between running and reference generator speed), the generator speed increment V_i and pitch angle control value θ as the linguistic variables. V_e and V_i are inputs of the fuzzy controller, θ is the controller output value. The linguistic values of V_e and θ both are:[NB NM NS ZO PS PM PB], which means negative big, negative middle, negative small, zero, positive small, positive middle, and positive big respectively; The linguistic values of V_i are: [N Z P], that means negative, zero, positive. Standard triangular membership functions have been used for both the inputs and the output of the fuzzy controller. The control law of a fuzzy controller is represented by a set of heuristically chosen fuzzy rules. The designed fuzzy rules used in this paper are given in Table 1.

Table 1: Rule base for proposed fuzzy controller

θ		V_i		
		N	Z	P
V_e	NB	PB	PB	PM
	NM	PB	PM	PS
	NS	PM	PS	ZO
	ZO	PS	ZO	NS
	PS	ZO	NS	NM
	PM	NS	NM	NB
	PB	NM	NB	NB

Given the rules and membership functions, the fuzzy controller produces the crisp and continuous nonlinear input/output map, as shown in Figure 7.

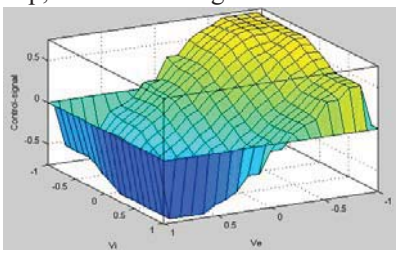

Figure 7: Fuzzy Controller Nonlinear Input & Output Map

The fuzzy map indicates that numerous nonlinearities are designed to enhance the controller's ability to drive the system to the set point. Soft and nonlinear control actions resulted from the fuzzy rules can improve the wind turbine performance [17]. An immediate and easy understanding of the controller logic can be obtained as following considerations:

1) If V_e is negative big and V_i is also negative, the output angle is too small and its amplitude is dropping, consequently current pitch angle must be fast increased.
2) If V_e is negative big while V_i is positive, the output is lower than its reference, but since its amplitude is increasing, pitch angle increment must be small.
3) If V_e is small, pitch angle variation must be smoothed because too large variations excite oscillatory modes [18].

To achieve global speed objective, the scroll air motor is controlled to achieve a specified output. In this application the PI-type control is used. Considering the limited volume of the scroll centre chamber, traditional PI valve displacement control is not quite efficient for scroll air motor. Proportional pressure regulator based PI control is applied to adjust the overall performance of the hybrid system. The PI control system in this study is depicted in Fig. 8,

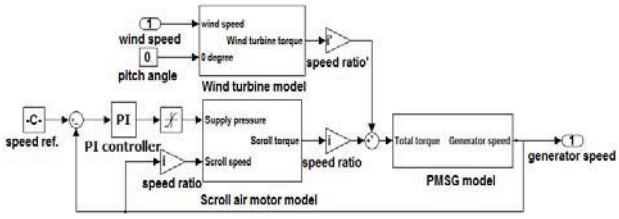

Figure 8: PI pressure controller diagram

The tracking error is defined as

$$e = \omega_{ref} - \omega_G \tag{27}$$

in which ω_{ref} represents the reference generator velocity. The PI control law can be represented as:

$$U = U_P + U_I = K_P e + K_I \int e \tag{28}$$

where U_P is a proportional controller; U_I is an integral controller; K_P and K_I are the corresponding control gains.

IV. Simulation Study

The considered 2 KW wind turbine is equipped with a three-blade rotor. Its parameters are shown in Table 2.

Table 2. Parameters of the simulated wind turbine

P_n	J_T	r_T	η	i
2 kw	4.9 kg × m^2	1.75 m	0.95	5

The scroll air motor employed is originated from the scroll compressor TRSA090. Besides, two simplicities have been assumed: infinite compressed air supply and continuous pitch angle change. The simulation considers the scenario when the input mean wind speed steps down within a 40 seconds' time series observation window, that is, drops from 10 m/s to 8 m/s at the time of 20 seconds. The wind speed curve is simulated based on Weibull distribution [19] (see Fig.9).

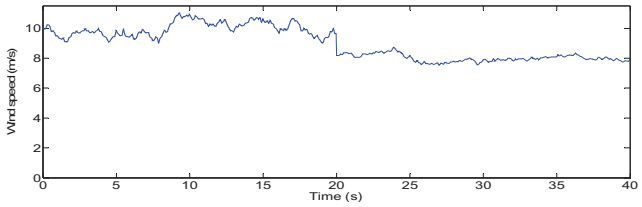

Figure 9: Input wind speed

For comparison, generator speeds from two different working conditions are demonstrated in one figure. They are: 1. stand-alone system without pneumatic actuators; 2. multi-mode controlled hybrid system, as shown in Fig.1.

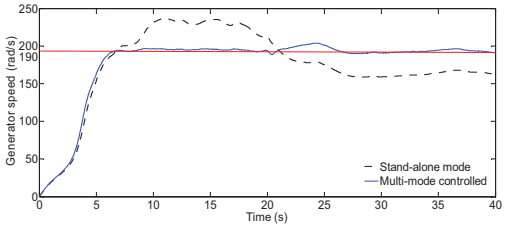

Figure 10: comparison of generator speeds in different working conditions

The target speed is set to 190 *rad/s*. From this figure, first, it can be concluded that the hybrid system can compensate

power efficiently during low wind speed. The generator can achieve additional torque input from pneumatic system. Moreover, we can see that the operation curves are almost the same at high wind speed, it reveals that there is few otiose load added by power transmission devices, mainly because of their relatively tiny inertias compared with the whole system's. Secondly, the multi-mode strategy performs well in close loop speed control, especially the fuzzy logical pitch control. The PI pressure control is not so effective, due to the highly nonlinear pressure dynamic characteristics resulted from the compressibility of air.

It is worth noting that this type of air motor should generally run with well-marked periodic fluctuation, which is originated from the cyclically changed chamber volume and pressure. That can be seen from the curve vibration during the air motor start stage in Fig. 11. Nonetheless, the air motor operates rather smoothly after it is engaged with the whole system, resulted from the large inertia load.

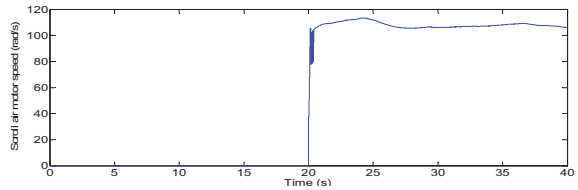

Figure 11: Scroll air motor speed curve in multi-mode control system

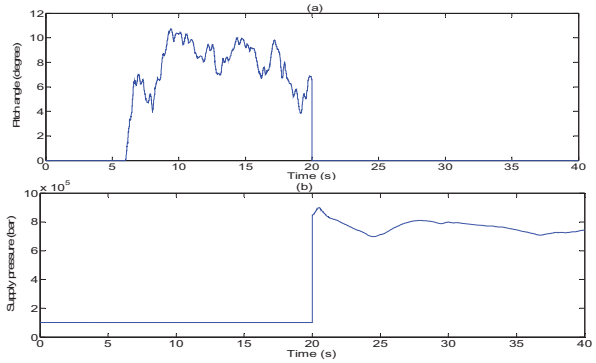

Figure 12: controlled variables curves in multi-mode control system

Fig.12 shows the controlled variables in multi-mode system. (a) is pitch angle value, which fluctuate to maintain a steady extracted wind power during high wind speed, and then decline to 0 degree for a maximum when wind speed is low. (b) describes the supply pressure curve. It starts to increase from 20 second, and then is controlled to adjust the compensated power from the pneumatic system.

V. Conclusion

A new concept of hybrid connection of a CAES to a small power scale wind turbine system is introduced in the paper. The complete process mathematical model and a multi-mode control strategy are derived and implemented in MATLAB/SIMULINK environment. The simulation results are very encouraging as the extra power from the scroll air motor output compensates the power shortfalls from wind energy. The control strategy proposed in the paper enables the hybrid wind turbine operates at a relatively steady speed profile, which in turn will improve the overall system reliability. The research project for the hybrid wind turbine system is still on-going and further improvement is expected to be reported in the near future.

References

[1]. World Wind Energy Association, [Online]. Available at: http://www.wwindea.org.

[2]. T. Gul, T. Stenzel, "Intermittency of wind: The wider picture," *Int. J. Global Energy Issues*, vol. 25, no. 3/4, pp. 163–186, 2006.

[3]. Taylor, J., Halnes, A., Analysis Of compressed air energy storage, *PCIC Europe 2010 Conference.*

[4]. A. Cavallo, "Controllable and affordable utility-scale electricity from intermittent wind resources and compressed air energy storage (CAES)", *Energy*, vol. 32, pp. 120-127, 2007.

[5]. S. Lemofouet, and A. Rufer, "A hybrid energy storage system based on compressed air and supercapacitors with maximum efficiency point tracking (MEPT)", *IEEE Transactions on Industrial Electronics*, vol. 53, No.4, pp. 1105-1115, 2006.

[6]. S. Van der Linden, "Bulk energy storage potential in the USA, current developments and future prospects", *Energy*, vol. 31, pp. 3446-3457, 2006.

[7]. H. Sun, J. Wang, S. Guo and X. Luo, "Study on Energy Storage Hybrid Wind Power Generation Systems", *World Congress on Engineering 2010*, London.

[8]. S. Heier, "Grid integration of Wind Energy Conversion Systems", *Chichester, UK John Wiley& Sons Ltd*., 1998.

[9]. L. Mihet-Popa, F. Blaabjerg, and I. Boldea, "Wind Turbine Generator Modeling and Simulation Where Rotational Speed is the Controlled Variable", *IEEE Transactions on Industry applications*, vol. 40, No. 1, January/February, 2004.

[10]. P. Pillay and R. Krishnan, "Modeling, simulation and analysis of permanent magnet motor drives, part 1: The permanent-magnet synchronous motor drive," *IEEE Trans. Ind. Applicat*., vol. 25, pp. 265–273, Mar./Apr. 1989.

[11]. J. Wang, L. Yang, X. Luo, S. Mangan, J.W. Derby, "Mathematical modelling study of scroll air motors and energy efficiency analysis - Part I", *IEEE/ASME Trans. on Mechatronics*, Vol. 16, No. 1, pp 112-121, 2011.

[12]. J. Wang, X. Luo, L. Yang, L Shpanin, S. Mangan, J.W. Derby, "Mathematical modelling study of scroll air motors and energy efficiency analysis - Part II", *IEEE/ASME Trans. on Mechatronics*, Vol. 16, No. 1. pp122- 132, 2011.

[13]. L. Yang, J. Wang, N. Lu, S. Mangan, and J.M. Derby, Energy efficiency analysis of a scroll-type air motor based on a simplified mathematical model, *The Proceedings of World Congress of Engineering* 2007, pp759-764, London, UK, June, 2007.

[14]. Y. P. B. Yeung, K. W. E. Cheng, W. W. Chan, C.Y. Lam, W. F. Choi, and T. W. Ng, "Automobile hybrid air conditioning technology," *The Proceedings of the 3rd International Conference on Power Electronics Systems and Application*s, pp116-116, 2009.

[15]. J. L. Wei, J. Wang, Q. H. Wu, G. Oluwanda, and M. Boardman, "Development of a multi-segment coal mill model using an evolutionary computation technique", *IEEE Transactions on Energy Conversion*, Vol. 22, pp718-727, 2007.

[16]. Wei, J.L. Wang, J and Wu, Q.H., Study of Three Different Approaches for Development of Power System Aggregated Load Area Models, *The Proceedings of American Control Conference 2008*, June 11-12, Seattle, USA, 2008.

[17]. Prats, M.A.M., Carrasco, J.M., Galvan, E., Sanchez, J.A., Franquelo, L.G., Batista, C., Improving transition between power optimization and power limitation of variable speed, variable pitch wind turbines using fuzzy control techniques, *Industrial Electronics Society, 2000. IECON 2000. 26th Annual Conference of the IEEE*.

[18]. Zhang, J., Cheng, M., Chen, Z., Fu, X., Pitch Angle Control for Variable Speed Wind Turbines, *DRPT2008 6-9 April 2008 Nanjing China*.

[19]. Yeh, T. H. and Wang, L. "A study on generator capacity for wind turbines under various tower heights and rated wind speeds using Weibull distribution," *IEEE Trans. Energy Convers.*, vol. 23, no. 2, pp. 592–602.